

Massive Scalar Corrections to Gravitational Potentials in the On-Shell Renormalization Scheme

Duojie Jimu^{1,*} and Tomislav Prokopec^{1,†}

¹*Institute for Theoretical Physics, Spinoza Institute & EMMEΦ,
Utrecht University, Princetonplein 5, 3584 CC Utrecht, The Netherlands*

We calculate the one-loop corrections induced by a non-minimally coupled massive scalar to the two gravitational potentials sourced by a static point mass in Minkowski space via solving the effective Einstein field equations. We first obtain a manifestly transverse graviton self-energy and, by performing resummation of the bubble diagrams, derive the associated dressed graviton propagator in the general covariant gauge. For one class of gauges, which include the Landau gauge, the dressed graviton propagator becomes proportional to the tree-level propagator in the on-shell limit. This fact allows us to employ the on-shell renormalization scheme so that the renormalized Newton constant G takes the value measured in the experiments. The resulting corrections to the gravitational potentials share similar structures with the vacuum polarization correction to the Coulomb potential regarding their analytic expressions and long distance behavior. By comparing our results with gravitational slip measurements, we establish a constraint on the non-minimal coupling: $|\xi| \lesssim 5 \times 10^{43}/\sqrt{N}$, where N is the number of scalar fields.

I. INTRODUCTION

Though the quantum behavior of gravity in the high energy regime is currently unclear, it is viable to study the low-energy, long-range quantum effects within a gravity-matter system by treating general relativity (GR) as a quantum field theory (QFT), as exemplified by the abundant studies on the quantum corrections to gravitational potentials induced by the loop effects of various particles [1–11]. The approaches employed in these studies mainly fall into two categories.

The first one, the *inverse scattering method*, is coupling two scalars with masses m_1 and m_2 to gravity, computing the amplitude of their scattering process, and using Born approximation to Fourier transform the scattering amplitude in the manner,

$$V(x) = \int \frac{d^3k}{(2\pi)^3} e^{i\vec{k}\cdot\vec{x}} \frac{i\mathcal{M}(\vec{k})}{2E_1 2E_2}, \quad (1)$$

to get the gravitational potential energy. Here E_1 and E_2 are the energies of the two scalars, $\mathcal{M}(\vec{k})$ is the scattering amplitude, and \vec{k} is the momentum transfer. In the non-relativistic limit, $E_1 \rightarrow m_1$ and $E_2 \rightarrow m_2$. This method was used in [1] to calculate the correction to $V(x)$ induced by graviton loops. See also [2] for the corrections induced by conformal fields with spin 0, 1/2 and 1, and [3] for those induced by massive fields with spin 0, 1/2 and 1. One virtue of this approach is its explicit gauge-independence through the use of S-matrix. Also, it can treat different species of massless particles on a different basis regarding how they experience gravitation (in contrast to the equivalence principle which claims all massless particles follow the same geodesic) [13–16]. However, this approach has its limitations as it is not known how to apply it to curved spacetimes where there are no well-defined *in* or *out* states.

An alternative approach [6, 7, 9] is deriving the quantum effective action and solving the resulting effective Einstein field equations, with other ingredients of GR such as the equivalence principle preserved. For example, when graviton interacts with quantum matter and develops a self-energy, the linearized effective Einstein field equations on a flat background take the form,

$$-\mathcal{L}_{\mu\nu\rho\sigma}\kappa h^{\rho\sigma}(x) - \int d^4x' [\mu\nu\Sigma_{\rho\sigma}](x;x')\kappa h^{\rho\sigma}(x') + \mathcal{O}((\kappa h^{\rho\sigma})^2) = 8\pi GT_{\mu\nu}(x). \quad (2)$$

Here $\kappa h^{\mu\nu}$ is the perturbation to the background metric, $\kappa = \sqrt{16\pi G}$ is the gravitational coupling constant and G is the Newton constant. The first term on the left is the linearized Einstein tensor, while the second term is

*Electronic address: jm.dj@outlook.com

†Electronic address: T.Prokopec@uu.nl

the quantum correction which involves integration of the retarded graviton self-energy $[\![_{\mu\nu}\Sigma_{\rho\sigma}]](x;x')$ against the metric perturbation $\kappa h^{\rho\sigma}(x')$. This equation is used in [4] to compute the one-loop corrections to both of the two gravitational potentials $\Phi(x)$ and $\Psi(x)$ induced by a minimally coupled massless scalar in Minkowski space. The result is later generalized in [5] to a non-minimally coupled massless scalar with a time-dependent source, and in [6–9] to de Sitter space. See also [10] for an early calculation considering the corrections induced by a non-minimally coupled massless scalar to the potentials sourced by a finite-volume ball, where the quantum correction appears as an effective energy-momentum tensor in the field equations. Despite its viability in these many scenarios, this alternative approach also has limitations. For instance, the effective field equations only encode the information of the quantum corrections to the graviton n -point functions, but often the loops appearing in the Feynman diagrams describing a gravitational scattering process cannot all be viewed as a correction to the graviton n -point functions. In this case, one needs to carefully add these additional loop effects which dress the source and the observer to the effective field equations, otherwise the result will be gauge-dependent and thus no physical information can be extracted from it without further labor [12].

In this paper, we choose the effective field equation approach to calculate the one-loop corrections induced by a non-minimally coupled massive scalar to the two gravitational potentials $\Phi(x)$ and $\Psi(x)$ sourced by a static point mass in Minkowski space. Since in this case the quantum loop effects are fully contained in the graviton two-point function, we do not encounter the gauge issue mentioned above, apart from the trivial linear gauge dependence which can be solved by constructing the gauge invariant Bardeen potentials, as it was done in *e.g.* Ref. [5]. The correction to $\Phi(x)$ induced by a minimally coupled massive scalar was calculated in [3] in the $\overline{\text{MS}}$ scheme where the corrected potential contains terms that depend on the renormalization scale μ explicitly. This does not mean the potential, as an observable, is dependent on this arbitrary scale μ ; instead, it implies that the *renormalized* Newton constant $G(\mu)$ also runs with μ , which simply tells us how the coupling constant in the effective theory depends on the physical coupling constant measured in the experiments. That means that all these μ -dependencies cancel each other such that the measured potential is independent of μ . It would be therefore convenient to identify G with the one measured in the experiments and remove the explicit μ -dependent terms from the potentials, by adopting the *on-shell renormalization scheme*. To do this, we shall tune the Ricci scalar counterterm such that the dressed graviton propagator reduces to the tree-level propagator in the on-shell limit. While this procedure is guaranteed to work in QED, as the photon propagator has only one tensor structure, to show that it works in gravity is nontrivial due to the existence of two linearly independent tensor structures in the graviton propagator. Usually, the on-shell scheme also includes the renormalization of the mass and field strength of the scalar, but since they do not affect the gravitational potentials at the order we are working in, we skip these steps and focus on the renormalization of the gravity sector.

The structure of this paper is as follows. In Section II, we calculate the graviton self-energy which is responsible for the quantum corrections to gravitational potentials and introduce the counterterms used for renormalization. In Section III, we derive the dressed graviton propagator in the general covariant gauge, study its on-shell limit, and perform on-shell renormalization. In Section IV, we solve the linearized effective Einstein field equations for the quantum-corrected gravitational potentials. In Section V, we explore the structural similarities between the quantum corrections to gravitational potentials and those to the Coulomb potential. In Section VI, we compare our results with gravitational slip measurements and establish a constraint on the non-minimal coupling ξ . We summarize our results in Section VII.

Our conventions are as follows. We use $(-, +, +, +)$ for the metric signature. The Riemann tensor is defined as $R^\rho{}_{\sigma\mu\nu} = \partial_\mu\Gamma^\rho_{\nu\sigma} + \Gamma^\rho_{\mu\lambda}\Gamma^\lambda_{\nu\sigma} - (\mu \leftrightarrow \nu)$. The graviton field is defined as the perturbation to the inverse metric, *i.e.* $g^{\mu\nu}(x) = \eta^{\mu\nu} + \kappa h^{\mu\nu}(x)$, with $\kappa = \sqrt{16\pi G}$ and $\eta_{\mu\nu}$ being the Minkowski metric. We use natural units $\hbar = 1 = c$.

II. GRAVITON SELF-ENERGY

Our action contains the Einstein-Hilbert term plus a non-minimally coupled real massive scalar,

$$S = \frac{1}{16\pi G} \int d^D x \sqrt{-g} R + \int d^D x \sqrt{-g} \left(-\frac{1}{2} g^{\mu\nu} \partial_\mu \phi \partial_\nu \phi - \frac{1}{2} m^2 \phi^2 - \frac{1}{2} \xi R \phi^2 \right). \quad (3)$$

Similar to [17], our graviton field $h^{\mu\nu}$ is defined as the perturbation to the inverse metric ¹,

$$g^{\mu\nu} = \eta^{\mu\nu} + \kappa h^{\mu\nu}, \quad (4)$$

¹ Alternative ways of expanding the metric are $g_{\mu\nu} = \eta_{\mu\nu} + \kappa h_{\mu\nu}$ and $g_{\mu\nu} = (e^{\kappa h})_{\mu\nu}$. However, when correctly analyzed, all these expansions give physically equivalent answers, see *e.g.* Ref. [19].

where $\eta^{\mu\nu}$ is the Minkowski metric and $\kappa \equiv \sqrt{16\pi G}$. Indices are raised or lowered by $\eta_{\mu\nu}$, and the trace of $h_{\mu\nu}$ is denoted by $h \equiv h_{\mu\nu}\eta^{\mu\nu}$. To study one-loop effects of the scalar, we only need to expand the action to quadratic order in $h_{\mu\nu}$. The result is:

$$\begin{aligned}
S &= S_h + S_\phi + S_3 + S_4, \\
S_h &= \int d^D x \left[-\frac{1}{4} \partial_\alpha h_{\mu\nu} \partial^\alpha h^{\mu\nu} + \frac{1}{4} \partial_\mu h \partial^\mu h + \frac{1}{2} \partial_\mu h^{\mu\nu} (\partial^\alpha h_{\nu\alpha} - \partial_\nu h) \right], \\
S_\phi &= \int d^D x \left(-\frac{1}{2} \partial_\mu \phi \partial^\mu \phi - \frac{1}{2} m^2 \phi^2 \right), \\
S_3 &= -\frac{\kappa}{2} \int d^D x T_{\mu\nu}^{(\phi)} h^{\mu\nu}, \\
S_4 &= \frac{\kappa^2}{4} \int d^D x \left[\partial_\mu \phi \partial_\nu \phi h^{\mu\nu} h - \left(\frac{h^2}{4} + \frac{h_{\mu\nu} h^{\mu\nu}}{2} \right) (\partial_\mu \phi \partial^\mu \phi + m^2 \phi^2) + \xi \phi^2 h^{\mu\nu} \mathcal{L}_{\mu\nu\rho\sigma} h^{\rho\sigma} \right],
\end{aligned} \tag{5}$$

in which $T_{\mu\nu}^{(\phi)}$ denotes the energy-momentum tensor of the scalar field on Minkowski background,

$$T_{\mu\nu}^{(\phi)} = \partial_\mu \phi \partial_\nu \phi - \frac{\eta_{\mu\nu}}{2} (\partial_\alpha \phi \partial^\alpha \phi + m^2 \phi^2) + \xi \left[\eta_{\mu\nu} \partial^2 (\phi^2) - \partial_\mu \partial_\nu (\phi^2) \right], \tag{6}$$

and $\mathcal{L}_{\mu\nu\rho\sigma}$ is the flat space Lichnerowicz operator,

$$\mathcal{L}_{\mu\nu\rho\sigma} = \frac{1}{2} (\eta_{\mu\nu} \eta_{\rho\sigma} \partial^2 - \eta_{\rho\sigma} \partial_\mu \partial_\nu - \eta_{\mu\nu} \partial_\rho \partial_\sigma - \eta_{\mu(\rho} \eta_{\sigma)\nu} \partial^2 + 2\partial_{(\mu} \eta_{\nu)(\rho} \partial_{\sigma)}). \tag{7}$$

One can see that S_h is the quadratic action of graviton, S_ϕ is the action of a free scalar, S_3 and S_4 are the three-point and four-point interaction terms, where in S_4 we have dropped a term in the form $\xi \partial(\phi^2) h \partial h$, since its contribution to the one-loop Feynman diagrams vanishes.

The corrections to the potentials arise from the graviton self-energy given by the three diagrams shown in FIG. 1.

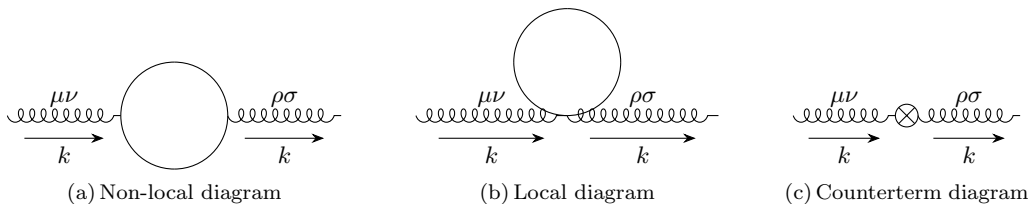


FIG. 1: Feynman diagrams contributing to the graviton self-energy. Coiled lines and solid lines represent graviton and the scalar, respectively.

By using the Feynman rules given in Appendix A, one can evaluate the amplitudes of diagrams (a) and (b) in FIG. 1 and add them together to give the primitive one-loop self-energy,

$$\begin{aligned}
-i[\mu\nu\Sigma_{\rho\sigma}] &= \kappa^2 \left[\frac{4(D-2)m^2 - (D^2 - 2D - 2)k^2}{16(D^2 - 1)} P_{\mu\nu} P_{\rho\sigma} + \frac{4(D-2)m^2 - k^2}{8(D^2 - 1)} P_{\mu\nu\rho\sigma} \right] I_1 \\
&+ \kappa^2 \left[\frac{(Dk^2 - 4m^2)^2 - 2(D+1)k^4}{32(D^2 - 1)} P_{\mu\nu} P_{\rho\sigma} + \frac{(k^2 + 4m^2)^2}{16(D^2 - 1)} P_{\mu\nu\rho\sigma} \right] I_2 \\
&+ \kappa^2 \xi \left[\frac{(D-3)k^2}{4(D-1)} P_{\mu\nu} P_{\rho\sigma} + \frac{k^2}{4} P_{\mu\nu\rho\sigma} \right] I_1 + \kappa^2 \xi \left[\frac{\xi k^4}{2} - \frac{(D-2)k^4}{4(D-1)} + \frac{m^2 k^2}{D-1} \right] P_{\mu\nu} P_{\rho\sigma} I_2 \\
&- \frac{\kappa^2 m^2}{4D} (\eta_{\mu\nu} \eta_{\rho\sigma} + 2\eta_{\mu(\rho} \eta_{\sigma)\nu}) I_1.
\end{aligned} \tag{8}$$

where the transverse projectors $P_{\mu\nu}$ and $P_{\mu\nu\rho\sigma}$ are defined as,

$$P_{\mu\nu} \equiv \eta_{\mu\nu} - \frac{k_\mu k_\nu}{k^2}, \quad P_{\mu\nu\rho\sigma} \equiv P_{\mu(\rho} P_{\sigma)\nu}, \tag{9}$$

and the integrals I_1 and I_2 are defined as,

$$\begin{aligned} I_1 &\equiv \int \frac{d^D p}{(2\pi)^D} \frac{1}{p^2 + m^2}, \\ I_2 &\equiv \int \frac{d^D p}{(2\pi)^D} \frac{1}{(p^2 + m^2)[(p+k)^2 + m^2]}. \end{aligned} \quad (10)$$

We see that, unlike the vacuum polarization in QED, the primitive graviton self-energy is not transverse due to the last term in (8). This can be traced back to the energy-momentum tensor of the scalar which can curve the space and spoil our flat space assumption, unless we introduce a specific cosmological constant to compensate for it. When the contribution from this cosmological constant is included, the primitive self-energy will become transverse, as we will see later.

The divergences in the primitive self-energy (8) can be removed by the following counterterms [20–22],

$$\Delta S = \int d^D x \sqrt{-g} (c_1 C_{\mu\nu\rho\sigma} C^{\mu\nu\rho\sigma} + c_2 R^2 + c_3 R + \Lambda), \quad (11)$$

with

$$\begin{aligned} c_1 &= \frac{\Omega \mu^{D-4}}{240(D-4)} + c_{1f}, \\ c_2 &= \frac{\Omega \mu^{D-4}}{4(D-4)} \left(\xi - \frac{1}{6} \right)^2 + c_{2f}, \\ c_3 &= \frac{\Omega m^2 \mu^{D-4}}{2(D-4)} \left(\xi - \frac{1}{6} \right) + c_{3f}, \\ \Lambda &= \frac{\Omega m^4}{4} \left(\frac{\mu^{D-4}}{D-4} + \Gamma_E - \frac{1}{4} \right). \end{aligned} \quad (12)$$

Here $C_{\mu\nu\rho\sigma}$ is the Weyl tensor, μ is an arbitrary energy scale introduced for dimensional regularization, and we used a shorthand notation,

$$\begin{aligned} \Omega &\equiv \frac{1}{8\pi^2}, \\ \Gamma_E &\equiv \frac{1}{2} \left[\ln \left(\frac{m^2}{4\pi\mu^2} \right) + \gamma_E - 1 \right]. \end{aligned} \quad (13)$$

In Eq. (12), c_{1f} , c_{2f} and c_{3f} are finite counterterms and their values depend on the choice of renormalization scheme. We keep them as free parameters for the moment and employ the on-shell renormalization scheme to put constraints on their values in the next section. The cosmological constant counterterm Λ is somewhat special as it is completely fixed. As mentioned above, in addition to removing the divergences, Λ also does the following jobs [3, 17]:

- (1) Its contribution to the expectation value of the total energy-momentum tensor cancels the one-loop contribution of the scalar field so that spacetime remains flat;
- (2) As another manifestation of (1), its one-point diagram cancels the tadpole diagram and ensures $\langle \hat{h}_{\mu\nu}(x) \rangle = 0$;
- (3) Its contribution to the graviton self-energy is essential for the latter to be transverse.

By using the Feynman rules given in Appendix A, we can evaluate the amplitude of the counterterm diagram in FIG. 1, combine it with the primitive self-energy (8), and reach the manifestly transverse, renormalized graviton self-energy,

$$-i[\mu\nu\Sigma_{\rho\sigma}] = i\kappa^2 A P_{\mu\nu} P_{\rho\sigma} + i\kappa^2 B Q_{\mu\nu\rho\sigma}, \quad (14)$$

with the transverse projector $Q_{\mu\nu\rho\sigma}$ defined as,

$$Q_{\mu\nu\rho\sigma} \equiv P_{\mu(\rho} P_{\sigma)\nu} - \frac{P_{\mu\nu} P_{\rho\sigma}}{D-1} \xrightarrow{D \rightarrow 4} P_{\mu(\rho} P_{\sigma)\nu} - \frac{P_{\mu\nu} P_{\rho\sigma}}{3}, \quad (15)$$

and the form factors given by:

$$A = -\frac{\Omega L(k^2)}{4} \left[k^2 \left(\xi - \frac{1}{6} \right) + \frac{m^2}{3} \right]^2 + k^4 \left[-\frac{\Omega(\Gamma_E + \frac{1}{2})}{2} \left(\xi - \frac{1}{6} \right)^2 + \frac{\Omega}{36} \left(\xi - \frac{1}{6} \right) + 2c_{2f} \right] + k^2 \left[-\frac{\Omega m^2 \Gamma_E}{6} \left(\xi - \frac{1}{6} \right) + \frac{\Omega m^2}{216} + \frac{c_{3f}}{3} \right], \quad (16)$$

$$B = -\frac{\Omega L(k^2)}{480} (k^2 + 4m^2)^2 + k^4 \left(-\frac{\Omega \Gamma_E}{240} + \frac{\Omega}{450} + c_{1f} \right) + k^2 \left[\frac{\Omega m^2 \Gamma_E}{4} \left(\xi - \frac{1}{6} \right) + \frac{\Omega m^2}{180} - \frac{c_{3f}}{2} \right],$$

in which $L(k^2)$, encoding the non-local effects, is defined as,

$$L(k^2) = \int_0^1 d\alpha \ln \left[1 + \frac{k^2}{m^2} \alpha(1-\alpha) \right] = -2 + \sqrt{1 + \frac{4m^2}{k^2}} \ln \left[\frac{\sqrt{1 + \frac{4m^2}{k^2}} + 1}{\sqrt{1 + \frac{4m^2}{k^2}} - 1} \right]. \quad (17)$$

In (17), the logarithm and square root should be understood as complex functions whose imaginary parts are uniquely fixed by the $i\epsilon$ prescription which can be restored by the substitution $k^2 \rightarrow k^2 - i\epsilon$. $P_{\mu\nu}P_{\rho\sigma}$ and $Q_{\mu\nu\rho\sigma}$ represent the spin-0 and spin-2 degrees of freedom of the propagator respectively. They satisfy the following identities:

$$P_{\mu\alpha}P^\alpha{}_\nu = P_{\mu\nu}, \quad P_{\mu\alpha}\eta^{\mu\alpha} = D-1, \quad Q_{\mu\nu\alpha\beta}Q^{\alpha\beta}{}_{\rho\sigma} = Q_{\mu\nu\rho\sigma}, \quad Q_{\mu\nu\rho\sigma}\eta^{\rho\sigma} = 0, \quad Q_{\mu\nu\rho\sigma}P^{\rho\sigma} = 0. \quad (18)$$

The property that $Q_{\mu\nu\rho\sigma}$ is orthogonal to $P_{\mu\nu}$ will simplify the contraction of indices when we compute the dressed graviton propagator in the next section.

III. DRESSED PROPAGATOR AND ON-SHELL RENORMALIZATION

In this section we first construct the one-loop dressed graviton propagator in the general covariant gauge (characterized by two real parameters). Then we show that for one class of gauges including the Landau gauge, the dressed graviton propagator is proportional to the tree-level propagator at the on-shell limit. This fact allows us to implement the on-shell renormalization scheme by tuning the finite part of the Ricci scalar counterterm. The on-shell scheme is convenient in the sense that the renormalized Newton constant would take the value measured in the experiments. Accordingly, our final result for the gravitational potentials (presented in Section IV) will not contain explicit μ -dependent terms, and we recover Newton's law of gravitation asymptotically at long distances.

A. General covariant gauge

To better understand the gauge dependence of the dressed propagator, we shall work in the general covariant gauge, which is obtained by adding the following gauge fixing action to the original action S_h in Eq. (5),

$$S_{\text{GF}}[h_{\mu\nu}] = \int d^D x \mathcal{L}_{\text{GF}}, \quad \mathcal{L}_{\text{GF}} = -\frac{1}{2\alpha} \left(\partial_\mu h^\mu{}_\gamma - \frac{\beta}{2} \partial_\gamma h \right) \eta^{\gamma\delta} \left(\partial_\nu h^\nu{}_\delta - \frac{\beta}{2} \partial_\delta h \right), \quad (19)$$

where $\alpha, \beta \in \mathbb{R}$ are real parameters. The resulting graviton propagator is derived as usual by calculating the inverse of the quadratic action and the result reads (in D dimensions) [12, 18],

$$i[\mu\nu\Delta_{\rho\sigma}^{(0)}] = \frac{2i}{k^2} \left\{ \frac{1}{(D-1)(D-2)} \left[P_{\mu\nu} - \frac{(D-1)\beta}{\beta-2} \frac{k_\mu k_\nu}{k^2} \right] \left[P_{\rho\sigma} - \frac{(D-1)\beta}{\beta-2} \frac{k_\rho k_\sigma}{k^2} \right] - Q_{\mu\nu\rho\sigma} - 2\alpha \frac{k_{(\mu} P_{\nu)(\rho} k_{\sigma)}}{k^2} - \frac{2\alpha}{(\beta-2)^2} \frac{k_\mu k_\nu k_\rho k_\sigma}{k^4} \right\}, \quad (20)$$

Once we have the tree-level propagator in hand, we can start computing the dressed propagator at one-loop order whose diagrammatic representation is given in FIG. 2.

$$i[\mu\nu\Delta_{\rho\sigma}^{(1)}] = \text{wavy line} + \text{wavy line with bubble} + \text{wavy line with two bubbles} + \dots$$

FIG. 2: The dressed propagator given by a summation over the bubble diagrams with increasing number of self-energy insertions. Every shaded circle (or “bubble”) represents an insertion of the graviton self-energy Eq. (14).

Let $\delta_n i[\mu\nu\Delta_{\rho\sigma}^{(1)}]$ denote the amplitude of the diagram with n self-energy insertions, namely the $(n+1)$ -th term in the summation in FIG. 2. Then by definition, we have:

$$i[\mu\nu\Delta_{\rho\sigma}^{(1)}] = \sum_{n=0}^{\infty} \delta_n i[\mu\nu\Delta_{\rho\sigma}^{(1)}]. \quad (21)$$

The tree-level graviton propagator (20) motivates the following *ansatz* for the dressed propagator:

$$\delta_n i[\mu\nu\Delta_{\rho\sigma}^{(1)}] = \frac{2i}{k^2} \left\{ a_n \left[P_{\mu\nu} - \frac{(D-1)\beta}{\beta-2} \frac{k_\mu k_\nu}{k^2} \right] \left[P_{\rho\sigma} - \frac{(D-1)\beta}{\beta-2} \frac{k_\rho k_\sigma}{k^2} \right] + b_n Q_{\mu\nu\rho\sigma} + c_n \frac{k_{(\mu} P_{\nu)(\rho} k_{\sigma)}}{k^2} + d_n \frac{k_\mu k_\nu k_\rho k_\sigma}{k^4} \right\}, \quad (22)$$

where a_n , b_n , c_n and d_n are some numerical factors. From Eqs. (14) and (20) the amplitude of the diagram with one more self-energy insertion, $\delta_{n+1} i[\mu\nu\Delta_{\rho\sigma}^{(1)}]$, is given by:

$$\begin{aligned} \delta_{n+1} i[\mu\nu\Delta_{\rho\sigma}^{(1)}] &= \delta_n i[\mu\nu\Delta_{\alpha\beta}^{(1)}] (-i[\alpha\beta\Sigma^{\tau\lambda}]) i[\tau\lambda\Delta_{\rho\sigma}^{(0)}] \\ &= \frac{2i}{k^2} \left\{ -\frac{2(D-1)\kappa^2}{(D-2)k^2} A a_n \left[P_{\mu\nu} - \frac{(D-1)\beta}{\beta-2} \frac{k_\mu k_\nu}{k^2} \right] \left[P_{\rho\sigma} - \frac{(D-1)\beta}{\beta-2} \frac{k_\rho k_\sigma}{k^2} \right] \right. \\ &\quad \left. + \frac{2\kappa^2}{k^2} B b_n Q_{\mu\nu\rho\sigma} - \delta_{n,0} 2\alpha \frac{k_{(\mu} P_{\nu)(\rho} k_{\sigma)}}{k^2} - \delta_{n,0} \frac{2\alpha}{(\beta-2)^2} \frac{k_\mu k_\nu k_\rho k_\sigma}{k^4} \right\}. \end{aligned} \quad (23)$$

To reach the last equality, we used the identities in Eq. (18) and the transversality of $P_{\mu\nu}$ and $Q_{\mu\nu\rho\sigma}$ repeatedly. Comparing this result with our *ansatz* (22), we find simple recurrence relations,

$$a_{n+1} = -\frac{2(D-1)\kappa^2}{(D-2)k^2} A a_n, \quad b_{n+1} = \frac{2\kappa^2}{k^2} B b_n. \quad (24)$$

The summation in Eq. (21) is thus a simple geometric series. Reading off $a_0 = \frac{1}{(D-1)(D-2)}$ and $b_0 = -1$ from Eq. (20), we can write down the dressed graviton propagator,

$$\begin{aligned} i[\mu\nu\Delta_{\rho\sigma}^{(1)}] &= \frac{2i}{k^2} \left[\frac{1}{(D-1)(D-2)} \frac{1}{1 + \frac{2(D-1)\kappa^2}{(D-2)k^2} A} \left(P_{\mu\nu} - \frac{(D-1)\beta}{\beta-2} \frac{k_\mu k_\nu}{k^2} \right) \left(P_{\rho\sigma} - \frac{(D-1)\beta}{\beta-2} \frac{k_\rho k_\sigma}{k^2} \right) - \frac{1}{1 - \frac{2\kappa^2}{k^2} B} Q_{\mu\nu\rho\sigma} \right. \\ &\quad \left. - 2\alpha \frac{k_{(\mu} P_{\nu)(\rho} k_{\sigma)}}{k^2} - \frac{2\alpha}{(\beta-2)^2} \frac{k_\mu k_\nu k_\rho k_\sigma}{k^4} \right]. \end{aligned} \quad (25)$$

This is the first main result of this work. We derived its form in general D dimensions to facilitate its application to other research, while for our purpose we take $D \rightarrow 4$ from now on. We see that $k^2 = 0$ is a pole of the dressed propagator. Moreover, it is a simple pole since A/k^2 and B/k^2 remain finite when $k^2 \rightarrow 0$, as can be seen from Eqs. (27) and (28). Therefore, graviton stays massless at one loop. However, additional poles do exist for non-perturbatively large momenta [24]. For completeness, we discuss these poles in Appendix B.

B. On-shell renormalization

To implement the on-shell renormalization scheme, we need to study the on-shell limit of the dressed propagator and tune the counterterms such that it reduces to the tree-level propagator in this limit. For this aim, we first study the limits of the function $L(k^2)$. By its definition in Eq. (17), we have:

$$\lim_{k^2 \rightarrow 0} L(k^2) k^2 = 0, \quad \lim_{k^2 \rightarrow 0} L(k^2) = 0, \quad \lim_{k^2 \rightarrow 0} \frac{L(k^2)}{k^2} = \int_0^1 d\alpha \frac{\alpha(1-\alpha)}{m^2} = \frac{1}{6m^2}. \quad (26)$$

Using these results and the expressions of A, B given in Eq. (16), we can evaluate the limits,

$$\begin{aligned} \lim_{k^2 \rightarrow 0} \frac{A}{k^2} &= \lim_{k^2 \rightarrow 0} \left\{ -\frac{\Omega L(k^2)}{4k^2} \left[k^2 \left(\xi - \frac{1}{6} \right) + \frac{m^2}{3} \right]^2 + k^2 \left[-\frac{\Omega(\Gamma_E + \frac{1}{2})}{2} \left(\xi - \frac{1}{6} \right)^2 + \frac{\Omega}{36} \left(\xi - \frac{1}{6} \right) + 2c_{2f} \right] \right. \\ &\quad \left. + \left[-\frac{\Omega m^2 \Gamma_E}{6} \left(\xi - \frac{1}{6} \right) + \frac{\Omega m^2}{216} + \frac{c_{3f}}{3} \right] \right\} \\ &= \lim_{k^2 \rightarrow 0} \left\{ -\frac{\Omega L(k^2)}{4k^2} \frac{m^4}{9} + \left[-\frac{\Omega m^2 \Gamma_E}{6} \left(\xi - \frac{1}{6} \right) + \frac{\Omega m^2}{216} + \frac{c_{3f}}{3} \right] \right\} \\ &= -\frac{\Omega m^2 \Gamma_E}{6} \left(\xi - \frac{1}{6} \right) + \frac{c_{3f}}{3}, \end{aligned} \quad (27)$$

and

$$\begin{aligned} \lim_{k^2 \rightarrow 0} \frac{B}{k^2} &= \lim_{k^2 \rightarrow 0} \left\{ -\frac{\Omega L(k^2)}{480k^2} (k^2 + 4m^2)^2 + k^2 \left(-\frac{\Omega \Gamma_E}{240} + \frac{\Omega}{450} + c_{1f} \right) + \left[\frac{\Omega m^2 \Gamma_E}{4} \left(\xi - \frac{1}{6} \right) + \frac{\Omega m^2}{180} - \frac{c_{3f}}{2} \right] \right\} \\ &= \lim_{k^2 \rightarrow 0} \left\{ -\frac{\Omega L(k^2)}{480k^2} 16m^4 + \left[\frac{\Omega m^2 \Gamma_E}{4} \left(\xi - \frac{1}{6} \right) + \frac{\Omega m^2}{180} - \frac{c_{3f}}{2} \right] \right\} \\ &= \frac{\Omega m^2 \Gamma_E}{4} \left(\xi - \frac{1}{6} \right) - \frac{c_{3f}}{2}. \end{aligned} \quad (28)$$

This means that the two form factors in the dressed propagator (25) have identical limits (after taking $D \rightarrow 4$),

$$Z(\mu) \equiv \lim_{k^2 \rightarrow 0} \frac{1}{1 + \frac{3\kappa^2}{k^2} A} = \lim_{k^2 \rightarrow 0} \frac{1}{1 - \frac{2\kappa^2}{k^2} B} = \frac{1}{1 + \kappa^2 \left[-\frac{\Omega m^2 \Gamma_E}{2} \left(\xi - \frac{1}{6} \right) + c_{3f} \right]}, \quad (29)$$

such that, for $\alpha = 0$ gauges, including the Landau gauge ($\alpha, \beta = 0$) [23], we have ²:

$$i[\mu\nu\Delta_{\rho\sigma}^{(1)}]_{\alpha=0} \xrightarrow{k^2 \rightarrow 0} Z(\mu) \times i[\mu\nu\Delta_{\rho\sigma}^{(0)}]_{\alpha=0}. \quad (30)$$

Remarkably, even though two tensor structures exist in the graviton propagator, the dressed one is proportional to the tree-level one in the on-shell limit, constituting the second important result of this paper. On-shell scheme then requires choosing c_{3f} such that $Z(\mu) = 1$, which corresponds to,

$$c_{3f} = \frac{\Omega m^2 \Gamma_E}{2} \left(\xi - \frac{1}{6} \right). \quad (31)$$

This can be viewed as a μ -dependent graviton wave function renormalization, or equivalently, a finite renormalization of the Newton constant.

In fact, we can derive $Z(\mu)$ directly using the renormalization group equation (RGE) without performing the resummation of the bubble diagrams in FIG. 2. This approach will also provide an alternative way to implement the on-shell scheme. Let us set c_{3f} to zero for the moment. From the divergent Ricci scalar counterterm given in Eq. (12), we can write down the relation between the bare Newton constant G_0 and the renormalized one G ,

$$\frac{1}{16\pi G_0} = \frac{1}{16\pi G} + \frac{\Omega m^2 \mu^{D-4}}{2(D-4)} \left(\xi - \frac{1}{6} \right). \quad (32)$$

The left-hand side is independent of μ , and therefore replacing $16\pi G$ with κ^2 and differentiating both sides with respect to μ gives,

$$0 = -\frac{1}{\kappa^4} \mu \frac{d\kappa^2}{d\mu} + \frac{\Omega m^2}{2} \left(\xi - \frac{1}{6} \right), \quad (33)$$

² The $\alpha = 0$ gauge is an exact gauge in which the condition (see Eq. (19)),

$$\partial_\mu h^\mu_\gamma - \frac{\beta}{2} \partial_\gamma h = 0,$$

is imposed. From Eq. (25) we see that for arbitrary α there are two additional vectorial pieces $\propto \alpha$ contributing to the dressed propagator. For scalar fields running in the loop these pieces are not dressed in the sense that they are the same as in the tree-level propagator.

from which we find the beta function of κ to the leading order (see *e.g.* [21]),

$$\mu \frac{d\kappa^2}{d\mu} = \frac{\kappa^4 \Omega m^2}{2} \left(\xi - \frac{1}{6} \right). \quad (34)$$

The solution of this equation reads,

$$\kappa^2(\mu) = \frac{\kappa_{\text{exp}}^2}{1 - \frac{\kappa_{\text{exp}}^2 \Omega m^2}{2} \left(\xi - \frac{1}{6} \right) \ln \left(\frac{\mu}{\mu_{\text{exp}}} \right)}, \quad (35)$$

where μ_{exp} and κ_{exp} are integration constants. For convenience, we let κ_{exp} equal to the value we measured in the experiments, *i.e.* $\kappa_{\text{exp}}^2/(16\pi) = G_{\text{exp}} \approx 6.67 \times 10^{-11} \text{ m}^3 \text{ kg}^{-1} \text{ s}^{-2}$, and μ_{exp} the corresponding renormalization scale. Expressing κ_{exp} in terms of κ yields,

$$\kappa_{\text{exp}}^2 = \frac{\kappa^2(\mu)}{1 + \frac{\kappa^2 \Omega m^2}{2} \left(\xi - \frac{1}{6} \right) \ln \left(\frac{\mu}{\mu_{\text{exp}}} \right)}. \quad (36)$$

Similar to QED, the relation between the physically measurable *effective* coupling constant, $\kappa_{\text{eff}}^2(k^2)$, and the unmeasurable *renormalized* one, $\kappa^2(\mu)$, can be read off from the dressed propagator³. In the $k^2 \rightarrow 0$ limit, it takes the form,

$$\kappa_{\text{eff}}^2(k^2 = 0) = \kappa^2(\mu) Z(\mu). \quad (37)$$

Moreover, $\kappa_{\text{eff}}^2(k^2 = 0)$ is nothing but κ_{exp}^2 , as κ_{exp}^2 is measured at macroscopic scales. Combining the above, we reach the expression of $Z(\mu)$,

$$Z(\mu) = \frac{\kappa_{\text{exp}}^2}{\kappa^2} = \frac{1}{1 + \frac{\kappa^2 \Omega m^2}{2} \left(\xi - \frac{1}{6} \right) \ln \left(\frac{\mu}{\mu_{\text{exp}}} \right)}. \quad (38)$$

Recall that $\Gamma_E \equiv \frac{1}{2} \left[\ln \left(\frac{m^2}{4\pi\mu^2} \right) + \gamma_E - 1 \right]$, we find Eqs. (38) and (29) are the same given that we make the following identification:

$$\mu_{\text{exp}}^2 = \frac{m^2}{4\pi} \exp \left[\gamma_E - 1 - \frac{4}{\Omega m^2 \left(\xi - \frac{1}{6} \right)} c_{3f} \right]. \quad (39)$$

From Eq. (35) we see how κ^2 (or equivalently $G = \kappa^2/(16\pi)$) varies with μ . From Eqs. (37)–(38) we observe that an alternative way to implement the on-shell scheme is to choose $\mu = \mu_{\text{exp}}$ so that $\kappa^2 = \kappa_{\text{exp}}^2$. This completes our procedure of on-shell renormalization.

Notice that c_{1f} and c_{2f} are still undetermined. This is a natural consequence of the fact that the Weyl tensor squared and the Ricci scalar squared do not affect the physics at low energies. Although this means there are still ambiguities regarding the k^4 terms in the self-energy, such ambiguities do not enter the gravitational potentials since k^4 terms in the self-energy give rise to delta function terms in the potentials, as can be seen from Eq. (59). As long as we restrict the applicability of our result to distances much larger than the Planck length, these delta function terms can be safely dropped.

If the scalar is massless, as is the case in [4, 5], we do not need the Ricci scalar counterterm at all, and the on-shell scheme is automatically realized.

Although c_{1f} and c_{2f} are not fixed, we can rewrite them to further simplify the self-energy. From Eqs. (12) and (31), we see the divergent and the finite parts of c_3 form a nice combination,

$$c_3 = c_{3\text{div}} + c_{3f} = \frac{\Omega m^2}{2} \left(\xi - \frac{1}{6} \right) \left(\frac{\mu^{D-4}}{D-4} + \Gamma_E \right). \quad (40)$$

³ However, when $k^2 \neq 0$, there seems no unique definition of $\kappa_{\text{eff}}^2(k^2)$ since the two form factors in the propagator are different. Even so, Eq. (37) holds not only to the zeroth order in the $k^2 \rightarrow 0$ limit, but to the *first* order, which means the correction to (37) for $0 < |k^2|/m^2 \ll 1$ is of $\mathcal{O}(k^4/m^4)$. This is because the first order term in the weak momentum expansion of the self-energy, being proportional to k^4 , corresponds to delta function terms in the potentials and therefore does not affect κ_{eff}^2 .

This form suggests that we recast c_{1f} and c_{2f} into the following form,

$$c_1 = \frac{\Omega}{240} \left(\frac{\mu^{D-4}}{D-4} + \Gamma_E \right) + c_{1x}, \quad c_2 = \frac{\Omega}{4} \left(\xi - \frac{1}{6} \right)^2 \left(\frac{\mu^{D-4}}{D-4} + \Gamma_E \right) + c_{2x}, \quad (41)$$

and thus,

$$c_{1f} = \frac{\Omega\Gamma_E}{240} + c_{1x}, \quad c_{2f} = \frac{\Omega\Gamma_E}{4} \left(\xi - \frac{1}{6} \right)^2 + c_{2x}. \quad (42)$$

We find that in this way all the Γ_E dependencies in the self-energy are nicely canceled. This phenomenon can be conveniently understood using the second approach to the on-shell scheme, *i.e.* by choosing $\mu = \mu_{\text{exp}}$, since with this choice of μ the Newton constant does not get dressed at one-loop order. The self-energy given by Eq. (14) and (16) now gets simplified to,

$$-i[\mu\nu\Sigma_{\rho\sigma}] = i\kappa^2 AP_{\mu\nu}P_{\rho\sigma} + i\kappa^2 BQ_{\mu\nu\rho\sigma}, \quad (43)$$

with

$$A = -\frac{\Omega L(k^2)}{4} \left[k^2 \left(\xi - \frac{1}{6} \right) + \frac{m^2}{3} \right]^2 + \left[-\frac{\Omega}{4} \left(\xi - \frac{1}{6} \right)^2 + \frac{\Omega}{36} \left(\xi - \frac{1}{6} \right) + 2c_{2x} \right] k^4 + \frac{\Omega m^2}{216} k^2, \quad (44)$$

$$B = -\frac{\Omega L(k^2)}{480} (k^2 + 4m^2)^2 + \left(\frac{\Omega}{450} + c_{1x} \right) k^4 + \frac{\Omega m^2}{180} k^2.$$

We note that in the computation of the $k^2 \rightarrow 0$ limit of A/k^2 and B/k^2 , the k^2 terms in the self-energy cancel the leading order contributions from the non-local, *i.e.* $L(k^2)$ dependent terms. As a result, the self-energy becomes local at energies much below the scalar mass. As pointed out in [25], this is a manifestation of the *decoupling* of the massive scalar in the infrared limit [26].

IV. SOLVING THE EFFECTIVE FIELD EQUATIONS

Having a fully renormalized graviton self-energy at hand, we can now derive and solve the linearized effective Einstein field equations for the quantum-corrected gravitational potentials. Our strategy is to first solve the equations in momentum space and then Fourier transform the solution to position space. The final result will be analytically expressed in terms of Bessel and Bickley functions.

A. Momentum space solution

The effective action in which the scalar degree of freedom has been integrated out takes the form,

$$\Gamma_h = S_h - \frac{1}{2} \int d^4x \int d^4x' h^{\mu\nu}(x) [\mu\nu\Sigma_{\rho\sigma}](x, x') h^{\rho\sigma}(x'). \quad (45)$$

Here S_h is the classical action of graviton given in Eq. (5). The effective equation of motion derived from the effective action in the presence of matter takes the form,

$$-\mathcal{L}_{\mu\nu\rho\sigma} \kappa h^{\rho\sigma}(x) - \int d^4x' [\mu\nu\Sigma_{\rho\sigma}](x, x') \kappa h^{\rho\sigma}(x') = \frac{\kappa^2}{2} T_{\mu\nu}(x), \quad (46)$$

in which $\mathcal{L}_{\mu\nu\rho\sigma}$ is given in Eq. (7). For the source of the potentials, we consider a static point particle with mass M at the origin. Thus,

$$T_{\mu\nu} = M\delta^3(\vec{x})\delta_\mu^0\delta_\nu^0. \quad (47)$$

We can then choose the Newtonian gauge in which the line element takes the form,

$$ds^2 = -(1 + 2\Phi)dt^2 + (1 - 2\Psi)(dx^2 + dy^2 + dz^2), \quad (48)$$

where Φ and Ψ are the two gravitational potentials.

We can solve Eq. (46) with ease in momentum space. Contrary to the computation of the dressed propagator, here it is slightly more convenient to use $P_{\mu\nu\rho\sigma}$ instead of $Q_{\mu\nu\rho\sigma}$. We hence rewrite the self-energy Eq. (43) as,

$$-i[\mu\nu\Sigma_{\rho\sigma}] = i\kappa^2\tilde{A}P_{\mu\nu}P_{\rho\sigma} + i\kappa^2\tilde{B}P_{\mu\nu\rho\sigma}, \quad (49)$$

where

$$\tilde{A} = A - \frac{B}{3}, \quad \tilde{B} = B. \quad (50)$$

The Fourier transform of the effective field equation Eq. (46) then takes the form,

$$\frac{k^2}{2}(P_{\mu\nu}P_{\rho\sigma} - P_{\mu\nu\rho\sigma})h^{\rho\sigma} + \kappa^2(\tilde{A}P_{\mu\nu}P_{\rho\sigma} + \tilde{B}P_{\mu\nu\rho\sigma})h^{\rho\sigma} = \kappa\pi M\delta(k^0)\delta_\mu^0\delta_\nu^0. \quad (51)$$

After some manipulations, the 00 component of Eq. (51) reads,

$$-\|\vec{k}\|^2\Psi + \kappa^2(\tilde{A} + \tilde{B})\frac{\|\vec{k}\|^4}{k^4}\Phi + \kappa^2\left[\tilde{A}\left(\frac{\|\vec{k}\|^2}{k^2} - 3\right) + \tilde{B}\frac{(k^0)^2}{k^2}\right]\frac{\|\vec{k}\|^2}{k^2}\Psi = \frac{\kappa^2\pi M}{2}\delta(k^0), \quad (52)$$

and the 11+22+33 component reads,

$$-\|\vec{k}\|^2\Phi + (-3(k^0)^2 + \|\vec{k}\|^2)\Psi + \kappa^2\left[\tilde{A}\left(\frac{\|\vec{k}\|^2}{k^2} - 3\right) + \tilde{B}\frac{(k^0)^2}{k^2}\right]\frac{\|\vec{k}\|^2}{k^2}\Phi + \kappa^2\left[\tilde{A}\left(\frac{\|\vec{k}\|^2}{k^2} - 3\right)^2 + \tilde{B}\left(\frac{(k^0)^4}{k^4} + 2\right)\right]\Psi = 0. \quad (53)$$

We can solve Eqs. (52) and (53) perturbatively. Expand the potentials in the form,

$$\Phi = \Phi^{(0)} + \kappa^2\Phi^{(1)} + \mathcal{O}(\kappa^4), \quad \Psi = \Psi^{(0)} + \kappa^2\Psi^{(1)} + \mathcal{O}(\kappa^4), \quad (54)$$

where the superscript (0) and (1) stand for the classical and quantum contributions, respectively. At the leading order, Eqs. (52) and (53) reduce to,

$$\begin{aligned} -\|\vec{k}\|^2\Psi^{(0)} &= \frac{\kappa^2\pi M}{2}\delta(k^0), \\ -\|\vec{k}\|^2\Phi^{(0)} + (-3(k^0)^2 + \|\vec{k}\|^2)\Psi^{(0)} &= 0, \end{aligned} \quad (55)$$

which have the following solution,

$$\Phi^{(0)} = \Psi^{(0)} = -\frac{\kappa^2\pi M}{2\|\vec{k}\|^2}\delta(k^0). \quad (56)$$

At the next-to-leading order, Eqs. (52) and (53) take the form,

$$\begin{aligned} -\|\vec{k}\|^2\Psi^{(1)} + (\tilde{A} + \tilde{B})\frac{\|\vec{k}\|^4}{k^4}\Phi^{(0)} + \left[\tilde{A}\left(\frac{\|\vec{k}\|^2}{k^2} - 3\right) + \tilde{B}\frac{(k^0)^2}{k^2}\right]\frac{\|\vec{k}\|^2}{k^2}\Psi^{(0)} &= 0, \\ -\|\vec{k}\|^2\Phi^{(1)} + (-3(k^0)^2 + \|\vec{k}\|^2)\Psi^{(1)} + \left[\tilde{A}\left(\frac{\|\vec{k}\|^2}{k^2} - 3\right) + \tilde{B}\frac{(k^0)^2}{k^2}\right]\frac{\|\vec{k}\|^2}{k^2}\Phi^{(0)} \\ + \left[\tilde{A}\left(\frac{\|\vec{k}\|^2}{k^2} - 3\right)^2 + \tilde{B}\left(\frac{(k^0)^4}{k^4} + 2\right)\right]\Psi^{(0)} &= 0. \end{aligned} \quad (57)$$

Thanks to the factor $\delta(k^0)$ in $\Phi^{(0)}$ and $\Psi^{(0)}$, we can take $\|\vec{k}\|^2/k^2 \rightarrow 1$ and $(k^0)^2/k^2 \rightarrow 0$ in Eq. (57), after which it can be readily solved to give,

$$\begin{aligned} \Phi^{(1)} &= \frac{\tilde{A} + 3\tilde{B}}{\|\vec{k}\|^2}\Phi^{(0)}, \\ \Psi^{(1)} &= \frac{-\tilde{A} + \tilde{B}}{\|\vec{k}\|^2}\Psi^{(0)}. \end{aligned} \quad (58)$$

Inserting Eqs. (56) and (58) into Eq. (54) and reverting back to the form factors without tilde through Eq. (50), we reach the Fourier transformed potentials,

$$\begin{aligned}\Phi(k) &= -\frac{\kappa^2 \pi M \delta(k^0)}{2\|\vec{k}\|^2} \left[1 + \frac{\kappa^2}{\|\vec{k}\|^2} \left(A + \frac{8}{3} B \right) \right], \\ \Psi(k) &= -\frac{\kappa^2 \pi M \delta(k^0)}{2\|\vec{k}\|^2} \left[1 - \frac{\kappa^2}{\|\vec{k}\|^2} \left(A - \frac{4}{3} B \right) \right].\end{aligned}\quad (59)$$

B. Reverting back to position space

The potentials in position space are given by the inverse Fourier transform,

$$\Phi(x) = \int \frac{d^4 k}{(2\pi)^4} e^{ik \cdot x} \Phi(k), \quad \Psi(x) = \int \frac{d^4 k}{(2\pi)^4} e^{ik \cdot x} \Psi(k). \quad (60)$$

To this end, we need the following identities,

$$\int \frac{d^3 k}{(2\pi)^3} e^{i\vec{k} \cdot \vec{x}} \frac{1}{\|\vec{k}\|^2} = \frac{1}{4\pi r}, \quad (61)$$

$$\int \frac{d^3 k}{(2\pi)^3} e^{i\vec{k} \cdot \vec{x}} L(\|\vec{k}\|^2) = -\frac{1}{2\pi r} J_0, \quad (62)$$

$$\int \frac{d^3 k}{(2\pi)^3} e^{i\vec{k} \cdot \vec{x}} \frac{L(\|\vec{k}\|^2)}{\|\vec{k}\|^2} = \frac{1}{2\pi r} J_1, \quad (63)$$

$$\int \frac{d^3 k}{(2\pi)^3} e^{i\vec{k} \cdot \vec{x}} \frac{L(\|\vec{k}\|^2)}{(\|\vec{k}\|^2)^2} = -\frac{1}{2\pi r} \left(J_2 - \frac{1}{12m^2} \right), \quad (64)$$

where $L(\|\vec{k}\|^2) = \int_0^1 d\alpha \ln \left[1 + \frac{\|\vec{k}\|^2}{m^2} \alpha(1-\alpha) \right]$ as we defined before and,

$$J_n(m, r) \equiv \int_{2m}^{\infty} dt \frac{\sqrt{t^2 - 4m^2}}{t^{2n}} e^{-rt}. \quad (65)$$

Eq. (61) is commonly used, so here we derive Eqs. (62), (63) and (64) by contour integration,

$$\begin{aligned}\int \frac{d^3 k}{(2\pi)^3} e^{i\vec{k} \cdot \vec{x}} \frac{L(\|\vec{k}\|^2)}{(\|\vec{k}\|^2)^n} &= \int \frac{d^3 k}{(2\pi)^3} \frac{e^{i\vec{k} \cdot \vec{x}}}{(\|\vec{k}\|^2)^n} \int_0^1 d\alpha \ln \left[1 + \frac{\|\vec{k}\|^2}{m^2} \alpha(1-\alpha) \right] \\ &= \frac{1}{(2\pi)^2} \int_0^1 d\alpha \int_0^\infty d\|\vec{k}\| \int_{-1}^1 d(\cos \theta) e^{i\|\vec{k}\| r \cos \theta} \|\vec{k}\|^{2-2n} \ln \left[1 + \frac{\|\vec{k}\|^2}{m^2} \alpha(1-\alpha) \right] \\ &= \frac{1}{(2\pi)^2 i r} \int_0^1 d\alpha \int_0^\infty d\|\vec{k}\| (e^{i\|\vec{k}\| r} - e^{-i\|\vec{k}\| r}) \|\vec{k}\|^{1-2n} \ln \left[1 + \frac{\|\vec{k}\|^2}{m^2} \alpha(1-\alpha) \right] \\ &= \frac{1}{(2\pi)^2 i r} \int_0^1 d\alpha \int_{-\infty}^\infty d\|\vec{k}\| e^{i\|\vec{k}\| r} \|\vec{k}\|^{1-2n} \ln \left[1 + \frac{\|\vec{k}\|^2}{m^2} \alpha(1-\alpha) \right].\end{aligned}\quad (66)$$

Now we take the trickiest $n = 2$ case as an example to illustrate the idea. The integrand possesses two branch cuts along the imaginary line due to the factor $\ln \left[1 + \frac{\|\vec{k}\|^2}{m^2} \alpha(1-\alpha) \right]$. It also has a pole at the origin due to the factor $\|\vec{k}\|^{-3}$. We thus consider the contour composed of $\gamma_1 \rightarrow \gamma_2 \rightarrow \dots \rightarrow \gamma_8$ shown in FIG. 3.

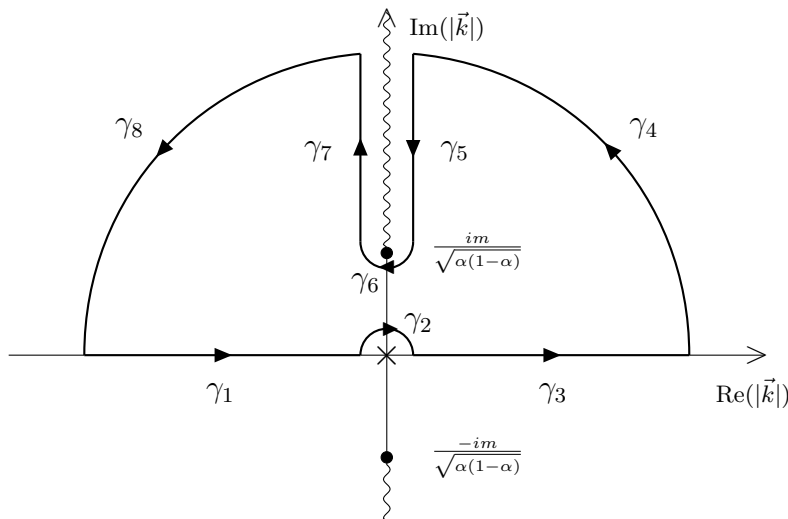


FIG. 3: The contour used to evaluate the $n = 2$ case of Eq. (66). It comprises eight pieces and bypasses both the branch cut along the imaginary line and the pole at the origin. γ_2 and γ_6 are infinitesimal semicircles. When $n = 0$ or $n = 1$, there's no pole at the origin so we do not need to curve the contour like γ_2 .

There is no pole enclosed in the whole contour, so the integral over it gives zero. This means Eq. (66), represented schematically as $\int_{\gamma_1+\gamma_3}$, is given by $-(\int_{\gamma_4+\gamma_8} + \int_{\gamma_5+\gamma_7} + \int_{\gamma_6} + \int_{\gamma_2})$. The contribution from the two arcs $\int_{\gamma_4+\gamma_8}$ vanishes due to the factor $e^{i\|\vec{k}\|r}$ in the integrand. \int_{γ_6} also vanishes since it scales as $\sim \rho \ln(\rho)$ where ρ is the radius of the semicircle. However, despite the size of γ_2 being infinitesimally small, \int_{γ_2} does not vanish, as the following computation shows:

$$\begin{aligned}
\int_{\gamma_2} \Big|_{n=2} &= \frac{1}{(2\pi)^2 i r} \int_0^1 d\alpha \int_{\gamma_2} d\|\vec{k}\| e^{i\|\vec{k}\|r} \frac{1}{\|\vec{k}\|^3} \ln \left[1 + \frac{\|\vec{k}\|^2}{m^2} \alpha(1-\alpha) \right] \\
&= \frac{1}{(2\pi)^2 i r} \int_0^1 d\alpha \lim_{\rho \rightarrow 0} \int_{\pi}^0 d\theta (i\rho e^{i\theta}) e^{i\rho e^{i\theta} r} \frac{1}{(\rho e^{i\theta})^3} \ln \left[1 + \frac{(\rho e^{i\theta})^2}{m^2} \alpha(1-\alpha) \right] \\
&= \frac{1}{(2\pi)^2 r} \int_0^1 d\alpha \lim_{\rho \rightarrow 0} \int_{\pi}^0 d\theta \frac{1}{\rho^2 e^{2i\theta}} \frac{(\rho e^{i\theta})^2}{m^2} \alpha(1-\alpha) \\
&= \frac{1}{(2\pi)^2 r} \int_0^1 d\alpha \frac{(-\pi)}{m^2} \alpha(1-\alpha) \\
&= -\frac{1}{24\pi m^2 r}.
\end{aligned} \tag{67}$$

Regarding the effect on the potentials, this contribution, stemming from the non-local part of the self-energy, will cancel those from the k^2 terms, which is a position space manifestation of the decoupling of the scalar we mentioned

earlier. Using $\ln(-|x| \pm i\epsilon) = \ln(|x|) \pm i\pi$ for $\epsilon \rightarrow 0^+$, we can evaluate $\int_{\gamma_5+\gamma_7}$ for a general n ,

$$\begin{aligned}
\int_{\gamma_5+\gamma_7} &= \frac{1}{(2\pi)^2 ir} \int_0^1 d\alpha \int_{\gamma_5+\gamma_7} d\|\vec{k}\| e^{i\|\vec{k}\|r} \|\vec{k}\|^{1-2n} \ln \left[1 + \frac{\|\vec{k}\|^2}{m^2} \alpha(1-\alpha) \right] \\
&= \frac{1}{(2\pi)^2 ir} \int_0^1 d\alpha \int_{\frac{im}{\sqrt{\alpha(1-\alpha)}}}^{i\infty} d\|\vec{k}\| e^{i\|\vec{k}\|r} \|\vec{k}\|^{1-2n} (-2i\pi) \\
&= \frac{(-1)^n}{2\pi r} \int_0^1 d\alpha \int_{\frac{m}{\sqrt{\alpha(1-\alpha)}}}^{\infty} dt e^{-tr} t^{1-2n} \\
&= \frac{(-1)^n}{2\pi r} \int_{2m}^{\infty} dt e^{-tr} t^{1-2n} \int_{\frac{1}{2}-\frac{1}{2}\sqrt{1-\frac{4m^2}{t^2}}}^{\frac{1}{2}+\frac{1}{2}\sqrt{1-\frac{4m^2}{t^2}}} d\alpha \\
&= \frac{(-1)^n}{2\pi r} \int_{2m}^{\infty} dt \frac{\sqrt{t^2-4m^2}}{t^{2n}} e^{-rt} \\
&= \frac{(-1)^n}{2\pi r} J_n(m, r),
\end{aligned} \tag{68}$$

where $J_n(m, r)$ is defined in Eq. (65). Combining the above results, we reach the identities Eqs. (62), (63) and (64).

Inserting the expressions of A and B given in Eq. (44) into Eq. (59), performing the transformation in Eq. (60) using the identities Eqs. (61), (62), (63) and (64), and neglecting the delta function terms as we argued earlier, we finally arrive at the result we have been looking for – the gravitational potentials sourced by a static point mass in the presence of a non-minimally coupled massive scalar in Minkowski space,

$$\begin{aligned}
\Phi(r) &= -\frac{GM}{r} \left\{ 1 + \frac{G}{\pi} \left[\left(\frac{1}{20} + \xi^2 - \frac{\xi}{3} \right) J_0 - m^2 \left(\frac{1}{15} + \frac{2\xi}{3} \right) J_1 + \frac{7m^4}{15} J_2 \right] \right\}, \\
\Psi(r) &= -\frac{GM}{r} \left\{ 1 - \frac{G}{\pi} \left[\left(\frac{1}{60} + \xi^2 - \frac{\xi}{3} \right) J_0 - m^2 \left(-\frac{1}{5} + \frac{2\xi}{3} \right) J_1 - \frac{m^4}{15} J_2 \right] \right\}.
\end{aligned} \tag{69}$$

The $\xi = 0$ limit of $\Phi(r)$ agrees with Eqs. (V.35) and (V.38) of [3], except for the absence of μ -dependent terms in our potentials, which can be traced back to on-shell renormalization.

Before we derive the analytic formula of $J_n(m, r)$, we can take the massless limit of our result. From the definition of $J_n(m, r)$ in Eq. (65), the massless limit of $J_0(m, r)$ reads,

$$J_0(0, r) = \frac{1}{r^2}. \tag{70}$$

Thus the massless limit of the potentials read,

$$\begin{aligned}
\Phi(r)|_{m^2=0} &= -\frac{GM}{r} \left[1 + \frac{G}{\pi r^2} \left(\frac{1}{20} + \xi^2 - \frac{\xi}{3} \right) \right], \\
\Psi(r)|_{m^2=0} &= -\frac{GM}{r} \left[1 - \frac{G}{\pi r^2} \left(\frac{1}{60} + \xi^2 - \frac{\xi}{3} \right) \right],
\end{aligned} \tag{71}$$

which agrees with [5, 10] precisely.

C. Analytic Expressions and Approximations

Now we evaluate the integral Eq. (65) following the approach of [27] which derived the analytic expression of the quantum-corrected Coulomb potential. This will facilitate our approximation of the potentials at long and short distances later. Define $z \equiv 2mr$. After a change of variable $t = 2m \cosh(x)$, Eq. (65) can be recast into the form,

$$J_n(m, r) = (2m)^{2-2n} \int_0^\infty dx \frac{\cosh^2(x) - 1}{\cosh^{2n}(x)} e^{-z \cosh(x)}. \tag{72}$$

For $J_0(m, r)$, using the following properties of the modified Bessel function of the second kind,

$$\begin{aligned} K_0(z) &= \int_0^\infty dx e^{-z \cosh(x)}, \\ K_0''(z) &= -\frac{K_1(z)}{z} + K_2(z), \\ K_1(z) &= -\frac{z}{2} [K_0(z) - K_2(z)], \end{aligned} \quad (73)$$

we get,

$$J_0(m, r) = (2m)^2 [K_0''(z) - K_0(z)] = (2m)^2 \frac{K_1(z)}{z}. \quad (74)$$

To evaluate $J_1(m, r)$ and $J_2(m, r)$, we introduce the Bickley function $\text{Ki}_n(z)$ which can be defined recursively as the integral of Bessel function [27],

$$\text{Ki}_0(z) \equiv K_0(z), \quad \text{and} \quad \text{Ki}_n(z) \equiv \int_z^\infty dz' \text{Ki}_{n-1}(z') \quad \text{for } n \geq 1. \quad (75)$$

$\text{Ki}_n(z)$ has an integral representation,

$$\text{Ki}_n(z) = \int_0^\infty dx \frac{e^{-z \cosh(x)}}{\cosh^n(x)}. \quad (76)$$

Comparing this with Eq. (72) gives,

$$J_n(m, r) = (2m)^{2-2n} [\text{Ki}_{2n-2}(z) - \text{Ki}_{2n}(z)], \quad (n \geq 1). \quad (77)$$

We thus have the following analytic expressions of the potentials:

$$\begin{aligned} \Phi(r) &= -\frac{GM}{r} \left\{ 1 + \frac{Gm^2}{\pi} \left[\left(\frac{1}{10} + 2\xi^2 - \frac{2\xi}{3} \right) \frac{K_1(2mr)}{mr} - \left(\frac{1}{15} + \frac{2\xi}{3} \right) (K_0(2mr) - \text{Ki}_2(2mr)) \right. \right. \\ &\quad \left. \left. + \frac{7}{60} (\text{Ki}_2(2mr) - \text{Ki}_4(2mr)) \right] \right\}, \\ \Psi(r) &= -\frac{GM}{r} \left\{ 1 - \frac{Gm^2}{\pi} \left[\left(\frac{1}{30} + 2\xi^2 - \frac{2\xi}{3} \right) \frac{K_1(2mr)}{mr} - \left(-\frac{1}{5} + \frac{2\xi}{3} \right) (K_0(2mr) - \text{Ki}_2(2mr)) \right. \right. \\ &\quad \left. \left. - \frac{1}{60} (\text{Ki}_2(2mr) - \text{Ki}_4(2mr)) \right] \right\}. \end{aligned} \quad (78)$$

Notice that the ξ -dependent quantum corrections contribute oppositely to the two potentials, such that the combination $\Phi(r) + \Psi(r)$ – responsible for the light bending studied in Refs. [13–16] – is independent of ξ . This is because, as one can see from Eq. (59), $\Phi(r) + \Psi(r)$ depends only on the spin-2 part of the self-energy (form factor B), while the non-minimal coupling ξ only affects the spin-0 part of the self-energy (form factor A), as Eq. (44) shows.

Given the analytic expressions of the potentials, we can study their long-distance and short-distance behavior conveniently. When $z \rightarrow \infty$, to sub-subleading order, we have the asymptotic forms,

$$\begin{aligned} K_n(z) &\sim \sqrt{\frac{\pi}{2z}} e^{-z} \left[1 + \frac{4n^2 - 1}{8z} + \frac{(4n^2 - 1)(4n^2 - 9)}{128z^2} \right], \\ \text{Ki}_n(z) &\sim \sqrt{\frac{\pi}{2z}} e^{-z} \left[1 - \frac{4n + 1}{8z} + \frac{3(16n^2 + 24n + 3)}{128z^2} \right]. \end{aligned} \quad (79)$$

Inserting this into Eq. (78), we get the long-distance approximation of the potentials,

$$\begin{aligned} \Phi(r)|_{r \rightarrow \infty} &= -\frac{GM}{r} \left\{ 1 + G\sqrt{\frac{m}{\pi r^3}} e^{-2mr} \left[\left(\xi - \frac{1}{4} \right)^2 + \frac{3}{16mr} \left(\xi - \frac{1}{4} \right) \left(\xi + \frac{13}{12} \right) \right] \right\}, \\ \Psi(r)|_{r \rightarrow \infty} &= -\frac{GM}{r} \left\{ 1 - G\sqrt{\frac{m}{\pi r^3}} e^{-2mr} \left[\left(\xi - \frac{1}{4} \right)^2 + \frac{3}{16mr} \left(\xi - \frac{1}{4} \right) \left(\xi + \frac{13}{12} \right) \right] \right\}. \end{aligned} \quad (80)$$

As promised, the potentials reduce to Newton's law of gravitation asymptotically. The $\xi = 0$ limit of $\Phi(r)|_{r \rightarrow \infty}$ does not agree with Eq. (V.57) of [3]. When our approximation method is applied to the quantum-corrected Coulomb potential, it gives the correct answer [27], giving credence to our result (80). Curiously, up to the order considered here, there is no quantum correction to the combination $\Phi(r)|_{r \rightarrow \infty} + \Psi(r)|_{r \rightarrow \infty}$, and the respective corrections to $\Phi(r)|_{r \rightarrow \infty}$ and $\Psi(r)|_{r \rightarrow \infty}$ vanish when $\xi = 1/4$.

When $z \rightarrow 0$, to subleading order, we have the asymptotic forms,

$$\begin{aligned} K_0(z) &\sim -\left[\ln\left(\frac{z}{2}\right) + \gamma_E\right] - \frac{z^2}{4}\left[\ln\left(\frac{z}{2}\right) + \gamma_E - 1\right], & \text{Ki}_2(z) &\sim 1 - \frac{\pi}{2}z, \\ K_1(z) &\sim \frac{1}{z} + \frac{z}{2}\left[\ln\left(\frac{z}{2}\right) + \gamma_E - \frac{1}{2}\right], & \text{Ki}_4(z) &\sim \frac{2}{3} - \frac{\pi}{4}z. \end{aligned} \quad (81)$$

In the same manner, we get the short-distance approximation of the potentials,

$$\begin{aligned} \Phi(r)|_{r \rightarrow 0} &= -\frac{GM}{r} \left\{ 1 + \frac{G}{\pi r^2} \left(\frac{1}{20} + \xi^2 - \frac{\xi}{3} \right) + \frac{Gm^2}{\pi} \left[\left(\frac{1}{6} + 2\xi^2 \right) (\ln(mr) + \gamma_E) + \frac{1}{18} - \xi^2 + \xi \right] \right\}, \\ \Psi(r)|_{r \rightarrow 0} &= -\frac{GM}{r} \left\{ 1 - \frac{G}{\pi r^2} \left(\frac{1}{60} + \xi^2 - \frac{\xi}{3} \right) - \frac{Gm^2}{\pi} \left[\left(-\frac{1}{6} + 2\xi^2 \right) (\ln(mr) + \gamma_E) - \frac{2}{9} - \xi^2 + \xi \right] \right\}. \end{aligned} \quad (82)$$

The $\xi = 0$ limit of $\Phi(r)|_{r \rightarrow 0}$ agrees with Eq. (V.60) of [3].

V. COMPARISON WITH THE UEHLING POTENTIAL

It is interesting to compare our gravitational potentials with the vacuum polarization correction to the Coulomb potential (usually called the Uehling potential), since in both cases the quantum corrections are induced by the loop effects of massive particles.

For a source with electric charge Q , the quantum-corrected Coulomb potential reads [27, 29],

$$\begin{aligned} \phi_C(r) &= \frac{Q}{4\pi r} \left(1 + \frac{e^2}{6\pi^2} \int_1^\infty dx e^{-2m_e r x} \frac{2x^2 + 1}{2x^4} \sqrt{x^2 - 1} \right) \\ &= \frac{Q}{4\pi r} \left[1 + \frac{e^2}{6\pi^2} \left(K_0(2m_e r) - \frac{1}{2}\text{Ki}_2(2m_e r) - \frac{1}{2}\text{Ki}_4(2m_e r) \right) \right], \end{aligned} \quad (83)$$

where m_e is the mass of electron. Using the identities (79), one can show that $\phi_C(r)$ has long-distance approximation,

$$\phi_C(r)|_{r \rightarrow \infty} = \frac{Q}{4\pi r} \left[1 + \frac{e^2}{16} \frac{e^{-2m_e r}}{(\pi m_e r)^{\frac{3}{2}}} \right], \quad (84)$$

and short-distance approximation,

$$\phi(r)|_{r \rightarrow 0} = \frac{Q}{4\pi r} \left[1 - \frac{e^2}{6} \left(\ln(m_e r) + \gamma_E + \frac{5}{6} \right) \right]. \quad (85)$$

Comparing these two expressions with Eqs. (80) and (82), we see that the long-distance behavior of the quantum corrections to the gravitational potentials and the Coulomb potential are of the same form, while at short distances, the correction to the gravitational potentials is stronger because of the $\sim 1/r^3$ terms.

VI. EXPERIMENTAL CONSTRAINTS

From Eq. (78) we see the quantum corrections to Φ and Ψ are different, which indicates a non-zero gravitational slip Σ defined as $\Sigma \equiv \Phi - \Psi$. Σ vanishes in GR and therefore serves as a probe for beyond-GR effects. Here we shall compare our theoretical prediction of Σ with the experimental results.

According to Eq. (80), the contributions to Σ from heavy scalars (those satisfying $mr \gg 1$ on solar system scales) exponentially decay at long distances and hence have no significance at macroscopic scales. We thus focus on the

effects of ultra-light and massless scalars, which have been proposed as dark matter [30–33] and dark energy [34–37] candidates. According to Eq. (71), such light scalars give rise to a non-zero gravitational slip,

$$\frac{\Sigma}{\Phi_0} = \frac{2G}{\pi r^2} \left(\xi^2 - \frac{\xi}{3} + \frac{1}{30} \right) + \frac{2Gm^2}{\pi} \left[2\xi^2 (\ln(mr) + \gamma_E) - \xi^2 + \xi - \frac{1}{12} \right], \quad (86)$$

where $\Phi_0 = \Psi_0 = -\frac{GM}{r}$ are the tree-level potentials. For ultra-light fields considered here the latter contribution is suppressed as $\sim -(mr)^2 \ln(mr) \ll 1$ and can thus be neglected. On the other hand, solar system tests have shown that [28],

$$\frac{\Sigma}{\Phi_0} < 2 \times 10^{-5}. \quad (87)$$

Combining the above two results, we obtain a constraint on the non-minimal coupling ξ ,

$$|\xi| < \sqrt{10\pi} \frac{r}{l_P} \times 10^{-3} \sim 5 \times 10^{43}, \quad (88)$$

where $l_P = \sqrt{G} = 1.6 \times 10^{-35}$ m is the Planck length and we took $r \approx 1.5 \times 10^{11}$ m which is the Sun-Earth distance. The constraint can be strengthened if the field is in a highly excited state, or if there is a large number of scalars running in the loop ($N \gg 1$). In the latter case, $|\xi| \lesssim 5 \times 10^{43} / \sqrt{N}$. In any case, the constraint is very weak; nevertheless, it is worth mentioning as it is a constraint established by perturbative quantum gravity through the investigation of the one-loop vacuum fluctuations of scalar matter in Minkowski space. To our knowledge, no such constraints have been claimed from loop effects in quantum gravity. We also note that it would be of interest to revisit the upper bound (88) for scalar fields in highly excited states, such as those generated during primordial inflation [34–38].

VII. CONCLUSION

In this work we calculate the one-loop corrections induced by a non-minimally coupled massive scalar to the two gravitational potentials Φ and Ψ sourced by a static point mass in Minkowski space. We choose here the effective field equation (2) approach to compute the quantum corrections, but we note that the inverse scattering method used in [1, 3] is equally suitable for this aim as long as one considers not only massive scalar-massive scalar scattering (to determine Φ), but also massive scalar-massless scalar scatterings (to determine $\Phi + \Psi$).

We have constructed a manifestly transverse graviton self-energy (43) by a particular choice of the cosmological constant counterterm (12). This counterterm ensures the flatness of the background spacetime and is essential for the transversality of the self-energy. The Ward identities involved in this scenario are studied in detail in [3].

To remove explicit μ -dependencies from the potentials, we adopt here the *on-shell renormalization scheme* in which the renormalized Newton constant G takes the value measured in the experiments and the potentials asymptotically reduce to Newton's law of gravitation in the long range limit. To implement the on-shell scheme, in Section III we first derive the dressed graviton propagator in the general covariant gauge by resumming the bubble diagrams shown in FIG. 2. We find that, for one class of exact gauges, which include the Landau gauge, the dressed graviton propagator becomes proportional to the tree-level propagator in the on-shell (or infrared) limit, with the ratio denoted by $Z(\mu)$ (29). This reveals a deep connection between the seemingly unrelated spin-0 and spin-2 parts of the graviton propagator – even though they are orthogonal to each other and possess different form factors, they share the same infrared limit dictated by the tree-level propagator. The on-shell scheme is then realized by tuning the Ricci scalar counterterm such that $Z(\mu) = 1$, which can be viewed as a finite graviton wave function renormalization, or equivalently, as a renormalization of the Newton constant. We also present another approach to on-shell renormalization, in which $Z(\mu)$ is derived from the renormalization group equation of the coupling constant $\kappa^2(\mu) = 16\pi G(\mu)$, and we simply fix μ at the point where $\kappa^2(\mu)$ reduces to its measured value κ_{exp}^2 .

In Section IV the resulting quantum-corrected gravitational potentials are expressed analytically in terms of Bessel functions and Bickley functions, in close analogy with the vacuum polarization correction to the Coulomb potential studied in [27]. Moreover, we find the corrections to these two kinds of potentials decay in the same manner at long distances, which corrects the result obtained in Ref. [3]. This suggests the universality of massive particle corrections to the long-range potential (long compared to the Compton wavelength of the massive particle) mediated by massless gauge bosons.

By comparing our results with gravitational slip measurements, in Section VI we establish an upper bound on the magnitude of the non-minimal coupling: $|\xi| \lesssim 5 \times 10^{43} / \sqrt{N}$, where N is the number of massless scalar fields. Even

though very weak, this constraint is to our knowledge the only known constraint on a coupling constant from the consideration of quantum gravitational loops.

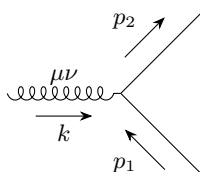
Finally, we note that the manifestly transverse graviton self-energy and the associated dressed graviton propagator in the general covariant gauge derived in this work can be used as the point of departure for other research.

Acknowledgments

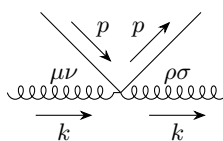
The authors thank Riley Kavanagh whose master's thesis [22] was used for various aspects of this work. This work is part of the Delta ITP consortium, a program of the Netherlands Organisation for Scientific Research (NWO) that is funded by the Dutch Ministry of Education, Culture and Science (OCW) — NWO project number 24.001.027.

Appendix A: Feynman Rules and Amplitudes

Here we give the intermediate steps in the derivation of the self-energy Eq. (14). From Eq. (5) we can read off the Feynman rules for the three-point and four-point vertices,



$$-i\kappa \left\{ p_1^{(\mu} p_2^{\nu)} - \frac{\eta^{\mu\nu}}{2} (p_1 \cdot p_2 + m^2) - \xi [\eta^{\mu\nu} (p_1 - p_2)^2 - (p_1 - p_2)^\mu (p_1 - p_2)^\nu] \right\}. \quad (\text{A1})$$



$$\frac{i\kappa^2}{2} \left[p^\mu p^\nu \eta^{\rho\sigma} + p^\rho p^\sigma \eta^{\mu\nu} - \left(\frac{1}{2} \eta^{\mu\nu} \eta^{\rho\sigma} + \eta^{\mu(\rho} \eta^{\sigma)\nu} \right) (p^2 + m^2) - \xi k^2 (P^{\mu\nu} P^{\rho\sigma} - P^{\mu\nu\rho\sigma}) \right]. \quad (\text{A2})$$

The momentum specification in the four-point vertex is not the most general one, but it suffices for our calculation at one-loop order. The amplitudes of diagrams (a) and (b) in FIG. 1 are then given by,

$$\begin{aligned} \mathcal{M}_{\mu\nu,\rho\sigma}^{(a)} &= \frac{1}{2} \int \frac{d^D p}{(2\pi)^D} (-i\kappa) \left\{ p_{(\mu} (p+k)_{\nu)} - \frac{\eta_{\mu\nu}}{2} [p \cdot (p+k) + m^2] - \xi k^2 P_{\mu\nu} \right\} \frac{-i}{p^2 + m^2} \\ &\quad \times \frac{-i}{(p+k)^2 + m^2} (-i\kappa) \left\{ p_{(\rho} (p+k)_{\sigma)} - \frac{\eta_{\rho\sigma}}{2} [p \cdot (p+k) + m^2] - \xi k^2 P_{\rho\sigma} \right\}, \end{aligned} \quad (\text{A3})$$

and

$$\mathcal{M}_{\mu\nu,\rho\sigma}^{(b)} = \frac{1}{2} \int \frac{d^D p}{(2\pi)^D} \frac{i\kappa^2}{2} \left[p_\mu p_\nu \eta_{\rho\sigma} + p_\rho p_\sigma \eta_{\mu\nu} - \left(\frac{1}{2} \eta_{\mu\nu} \eta_{\rho\sigma} + \eta_{\mu(\rho} \eta_{\sigma)\nu} \right) (p^2 + m^2) - \xi k^2 (P_{\mu\nu} P_{\rho\sigma} - P_{\mu\nu\rho\sigma}) \right] \frac{-i}{p^2 + m^2}. \quad (\text{A4})$$

After some strenuous manipulations, we can put them into the form,

$$\begin{aligned} \mathcal{M}_{\mu\nu,\rho\sigma}^{(a)} &= \kappa^2 \left[\frac{4(D-2)m^2 - (D^2 - 2D - 2)k^2}{16(D^2 - 1)} P_{\mu\nu} P_{\rho\sigma} + \frac{4(D-2)m^2 - k^2}{8(D^2 - 1)} P_{\mu\nu\rho\sigma} \right] I_1 \\ &\quad + \kappa^2 \left[\frac{(Dk^2 - 4m^2)^2 - 2(D+1)k^4}{32(D^2 - 1)} P_{\mu\nu} P_{\rho\sigma} + \frac{(k^2 + 4m^2)^2}{16(D^2 - 1)} P_{\mu\nu\rho\sigma} \right] I_2 \\ &\quad + \frac{\kappa^2 \xi (D-2)k^2}{2(D-1)} P_{\mu\nu} P_{\rho\sigma} I_1 + \kappa^2 \xi \left[\frac{\xi k^4}{2} - \frac{(D-2)k^4}{4(D-1)} + \frac{m^2 k^2}{D-1} \right] P_{\mu\nu} P_{\rho\sigma} I_2 \\ &\quad + \frac{\kappa^2 m^2}{4D} (\eta_{\mu\nu} \eta_{\rho\sigma} - 2\eta_{\mu(\rho} \eta_{\sigma)\nu}) I_1, \end{aligned} \quad (\text{A5})$$

and

$$\mathcal{M}_{\mu\nu,\rho\sigma}^{(b)} = -\frac{\kappa^2 m^2}{2D} \eta_{\mu\nu} \eta_{\rho\sigma} I_1 - \frac{\kappa^2 \xi k^2}{4} (P_{\mu\nu} P_{\rho\sigma} - P_{\mu\nu\rho\sigma}) I_1, \quad (\text{A6})$$

where the projectors $P_{\mu\nu}$ and $P_{\mu\nu\rho\sigma}$ are defined in Eq. (9), and the integrals I_1 and I_2 defined in Eq. (10) can be evaluated,

$$\begin{aligned} I_1 &= \int \frac{d^D p}{(2\pi)^D} \frac{1}{p^2 + m^2} = i\Omega m^2 \mu^{D-4} \left(\frac{1}{D-4} + \Gamma_E \right) + \mathcal{O}(D-4), \\ I_2 &= \int \frac{d^D p}{(2\pi)^D} \frac{1}{(p^2 + m^2)[(p+k)^2 + m^2]} = -i\Omega \mu^{D-4} \left(\frac{1}{D-4} + \Gamma_E + \frac{L(k^2) + 1}{2} \right) + \mathcal{O}(D-4). \end{aligned} \quad (\text{A7})$$

The shorthand notations Ω , Γ_E and $L(k^2)$ are defined in Eqs. (13) and (17). By expanding the counterterms in Eq. (11) to quadratic order in $h_{\mu\nu}$, we can find their contributions to diagram (c) in FIG. 1,

$$\begin{aligned} \mathcal{M}_{\mu\nu,\rho\sigma}^{(C^2)} &= \frac{2ic_1 \kappa^2 (D-3)}{D-2} k^4 \left(P_{\mu\nu\rho\sigma} - \frac{1}{D-1} P_{\mu\nu} P_{\rho\sigma} \right), \\ \mathcal{M}_{\mu\nu,\rho\sigma}^{(R^2)} &= 2ic_2 \kappa^2 k^4 P_{\mu\nu} P_{\rho\sigma}, \\ \mathcal{M}_{\mu\nu,\rho\sigma}^{(R)} &= \frac{ic_3 \kappa^2}{2} k^2 (P_{\mu\nu} P_{\rho\sigma} - P_{\mu\nu\rho\sigma}), \\ \mathcal{M}_{\mu\nu,\rho\sigma}^{(\Lambda)} &= \frac{i\Lambda \kappa^2}{4} (\eta_{\mu\nu} \eta_{\rho\sigma} + 2\eta_{\mu(\rho} \eta_{\sigma)\nu}). \end{aligned} \quad (\text{A8})$$

We see that, unlike other counterterm amplitudes, $\mathcal{M}_{\mu\nu,\rho\sigma}^{(\Lambda)}$ is not transverse, and indeed it cancels the non-transverse part of $\mathcal{M}_{\mu\nu,\rho\sigma}^{(a)} + \mathcal{M}_{\mu\nu,\rho\sigma}^{(b)}$ exactly. Combining the above amplitudes, one obtains the primitive self-energy (8), which after adding the counterterms (11)–(12) and taking the $D \rightarrow 4$ limit, yields the renormalized self-energy (14).

Appendix B: Pole Structure of the Dressed Graviton Propagator

In this appendix, we briefly study the pole structure of the dressed graviton propagator Eq. (25). For the impact of these poles on causality, unitarity and other properties of the theory, we refer the reader to Ref. [24]. For simplicity, we now assume the mass of the scalar to be small, *i.e.* we take $k^2/m^2 \rightarrow \infty$, so that we can find the poles analytically. In this limit, $L(k^2)$ given in Eq. (17) can be approximated by,

$$L(k^2) \simeq \ln \left(\frac{k^2}{m^2} \right) - 2. \quad (\text{B1})$$

Considering the self-energy Eq. 44 and restoring Γ_E through Eq. (42), the m^2 in $L(k^2)$ cancels those in Γ_E . Consequently, m^2 drops out and A , B become

$$\begin{aligned} A &\simeq -\frac{\Omega k^4}{4} \left\{ \left[\ln \left(\frac{k^2}{4\pi\mu^2} \right) + \gamma_E - 2 \right] \left(\xi - \frac{1}{6} \right)^2 - \frac{1}{9} \left(\xi - \frac{1}{6} \right) - \frac{8c_{2f}}{\Omega} \right\}, \\ B &\simeq -\frac{\Omega k^4}{480} \left[\ln \left(\frac{k^2}{4\pi\mu^2} \right) + \gamma_E - \frac{61}{15} - \frac{480c_{1f}}{\Omega} \right]. \end{aligned} \quad (\text{B2})$$

Let us first look at the poles of the spin-2 part of the dressed propagator. The poles other than the massless pole is determined by the condition,

$$1 - \frac{2\kappa^2}{k^2} B = 0, \quad (\text{B3})$$

which can be put into the form,

$$\ln(z) + \frac{1}{z} + \alpha = 0, \quad (\text{B4})$$

where the variable z and parameter α are defined as,

$$\begin{aligned} z &\equiv \frac{\kappa^2 \Omega}{240} k^2, \\ \alpha &\equiv \ln \left(\frac{60}{\kappa^2 \Omega \pi \mu^2} \right) + \gamma_E - \frac{61}{15} - \frac{480 c_{1f}}{\Omega}. \end{aligned} \quad (\text{B5})$$

This equation has two solutions given by the Lambert W function,

$$\begin{aligned} z_0 &= -\frac{1}{W_0(-e^\alpha)}, \\ z_{-1} &= -\frac{1}{W_{-1}(-e^\alpha)}. \end{aligned} \quad (\text{B6})$$

These two poles are real and positive for $\alpha \leq -1$ and form a complex-conjugate pair for $\alpha > -1$, as FIG. 4 shows.

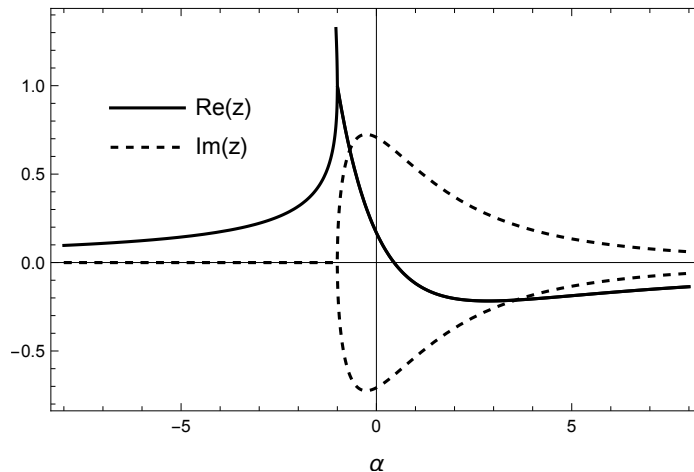


FIG. 4: The two poles of the spin-2 part of the dressed graviton propagator. Solid line and dashed line represent their real and imaginary parts, respectively. As $\alpha \rightarrow -\infty$, $z_{-1} \rightarrow 0$ while $z_0 \rightarrow \infty$. The two poles merge into one when $\alpha = -1$. One may compare this figure with Figure 14 of Ref. [24].

Next we study the pole structure of the spin-0 part of the dressed propagator. The poles are determined by the condition,

$$1 + \frac{3\kappa^2}{k^2} A = 0. \quad (\text{B7})$$

For a conformal scalar with $\xi = 1/6$, this equation becomes trivial,

$$1 + 6\kappa^2 c_{2f} k^2 = 0. \quad \left(\xi = \frac{1}{6} \right) \quad (\text{B8})$$

The pole only exists for $c_{2f} \neq 0$,

$$k^2 = -\frac{1}{6\kappa^2 c_{2f}}. \quad \left(\xi = \frac{1}{6} \text{ and } c_{2f} \neq 0 \right). \quad (\text{B9})$$

This is a real pole and its sign depends on c_{2f} . On the other hand, when $\xi \neq 1/6$, Eq. (B7) takes the form,

$$\ln(Z) - \frac{1}{Z} + \beta = 0, \quad (\text{B10})$$

where

$$\begin{aligned} Z &\equiv \frac{3\kappa^2 \Omega (\xi - \frac{1}{6})^2}{4} k^2, \\ \beta &\equiv \ln \left(\frac{1}{3\kappa^2 \Omega (\xi - \frac{1}{6})^2 \pi \mu^2} \right) + \gamma_E - 2 - \frac{1}{(\xi - \frac{1}{6})^2} \left(\frac{\xi - \frac{1}{6}}{9} + \frac{8c_{2f}}{\Omega} \right). \end{aligned} \quad (\text{B11})$$

This equation has only one solution given also by the Lambert W function,

$$Z_0 = \frac{1}{W_0(e^\beta)}. \quad \left(\xi \neq \frac{1}{6}\right) \quad (\text{B12})$$

This is a real positive pole for any value of β , as FIG. 5 shows. A pole within the range $Z_0 \gg 1$ are reached when $\beta < 0$, *i.e.* for sufficiently large (super-Planckian) scales $\mu \gg 1/\kappa$. These poles correspond to super-Planckian momenta ($k^2 \gg 1/\kappa^2$), and therefore are not perturbative and cannot be considered as physical. On the other hand, a pole at $Z_0 \ll 1$ are obtained when $1/\kappa \gg \mu \gg m$, *i.e.* for sufficiently small scales of μ . These poles correspond to sub-Planckian momenta, and thus could be physical (in the sense that they are not significantly affected by the higher order perturbative effects).

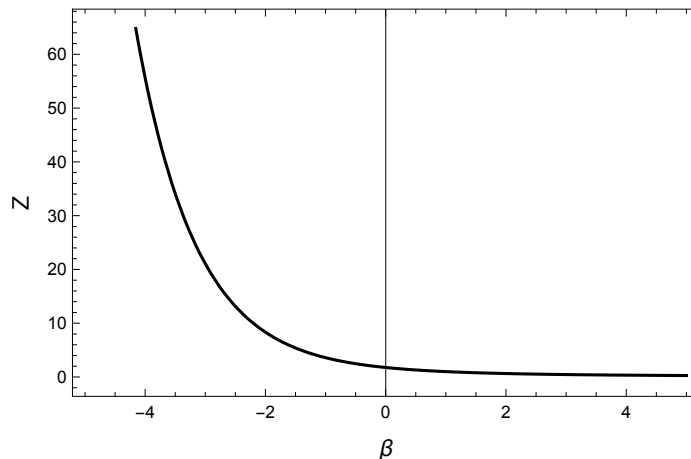


FIG. 5: The only pole of the spin-0 part of the dressed graviton propagator in the case of $\xi \neq 1/6$. It approaches zero asymptotically as β increases.

-
- [1] N. E. J. Bjerrum-Bohr, J. F. Donoghue and B. R. Holstein, “Quantum gravitational corrections to the nonrelativistic scattering potential of two masses,” *Phys. Rev. D* **67** (2003), 084033 [erratum: *Phys. Rev. D* **71** (2005), 069903] doi:10.1103/PhysRevD.71.069903 [arXiv:hep-th/0211072 [hep-th]].
 - [2] M. J. Duff and J. T. Liu, “Complementarity of the Maldacena and Randall-Sundrum pictures,” *Phys. Rev. Lett.* **85** (2000), 2052-2055 doi:10.1088/0264-9381/18/16/310 [arXiv:hep-th/0003237 [hep-th]].
 - [3] D. Burns and A. Pilaftsis, “Matter Quantum Corrections to the Graviton Self-Energy and the Newtonian Potential,” *Phys. Rev. D* **91** (2015) no.6, 064047 doi:10.1103/PhysRevD.91.064047 [arXiv:1412.6021 [hep-th]].
 - [4] S. Park and R. P. Woodard, “Solving the Effective Field Equations for the Newtonian Potential,” *Class. Quant. Grav.* **27** (2010), 245008 doi:10.1088/0264-9381/27/24/245008 [arXiv:1007.2662 [gr-qc]].
 - [5] A. Marunovic and T. Prokopec, “Time transients in the quantum corrected Newtonian potential induced by a massless nonminimally coupled scalar field,” *Phys. Rev. D* **83** (2011), 104039 doi:10.1103/PhysRevD.83.104039 [arXiv:1101.5059 [gr-qc]].
 - [6] C. L. Wang and R. P. Woodard, “One-loop quantum electrodynamic correction to the gravitational potentials on de Sitter spacetime,” *Phys. Rev. D* **92** (2015), 084008 doi:10.1103/PhysRevD.92.084008 [arXiv:1508.01564 [gr-qc]].
 - [7] S. Park, T. Prokopec and R. P. Woodard, “Quantum Scalar Corrections to the Gravitational Potentials on de Sitter Background,” *JHEP* **01** (2016), 074 doi:10.1007/JHEP01(2016)074 [arXiv:1510.03352 [gr-qc]].
 - [8] M. B. Fröb and E. Verdaguer, “Quantum corrections to the gravitational potentials of a point source due to conformal fields in de Sitter,” *JCAP* **03** (2016), 015 doi:10.1088/1475-7516/2016/03/015 [arXiv:1601.03561 [hep-th]].
 - [9] S. P. Miao, N. C. Tsamis and R. P. Woodard, “Alternate computation of gravitational effects from a single loop of inflationary scalars,” *JHEP* **07** (2024), 099 doi:10.1007/JHEP07(2024)099 [arXiv:2405.00116 [gr-qc]].
 - [10] A. Satz, F. D. Mazzitelli and E. Alvarez, “Vacuum polarization around stars: Nonlocal approximation,” *Phys. Rev. D* **71** (2005), 064001 doi:10.1103/PhysRevD.71.064001 [arXiv:gr-qc/0411046 [gr-qc]].
 - [11] S. P. Miao, N. C. Tsamis and R. P. Woodard, “Summing Gravitational Effects from Loops of Inflationary Scalars,” [arXiv:2405.01024 [gr-qc]].
 - [12] S. P. Miao, T. Prokopec and R. P. Woodard, “Deducing Cosmological Observables from the S-matrix,” *Phys. Rev. D* **96** (2017) no.10, 104029 doi:10.1103/PhysRevD.96.104029 [arXiv:1708.06239 [gr-qc]].

- [13] N. E. J. Bjerrum-Bohr, J. F. Donoghue, B. R. Holstein, L. Planté and P. Vanhove, “Bending of Light in Quantum Gravity,” *Phys. Rev. Lett.* **114** (2015) no.6, 061301 doi:10.1103/PhysRevLett.114.061301 [arXiv:1410.7590 [hep-th]].
- [14] N. E. J. Bjerrum-Bohr, J. F. Donoghue, B. R. Holstein, L. Plante and P. Vanhove, “Light-like Scattering in Quantum Gravity,” *JHEP* **11** (2016), 117 doi:10.1007/JHEP11(2016)117 [arXiv:1609.07477 [hep-th]].
- [15] D. Bai and Y. Huang, “More on the Bending of Light in Quantum Gravity,” *Phys. Rev. D* **95** (2017) no.6, 064045 doi:10.1103/PhysRevD.95.064045 [arXiv:1612.07629 [hep-th]].
- [16] H. H. Chi, “Graviton Bending in Quantum Gravity from One-Loop Amplitudes,” *Phys. Rev. D* **99** (2019) no.12, 126008 doi:10.1103/PhysRevD.99.126008 [arXiv:1903.07944 [hep-th]].
- [17] D. M. Capper, “On quantum corrections to the graviton propagator,” *Nuovo Cim. A* **25** (1975), 29 doi:10.1007/BF02735608.
- [18] D. M. Capper, “A general gauge graviton loop calculation,” *J. Phys. A* **13** (1980), 199 doi:10.1088/0305-4470/13/1/022
- [19] R. van Haasteren and T. Prokopec, “Scalar propagator for planar gravitational waves,” [arXiv:2204.12930 [gr-qc]].
- [20] G. Geist, H. Kuehnelt and W. Lang, “Invariant regularization of the one-meson loop in curved space-time,” *Nuovo Cim. A* **14** (1973), 103-116 doi:10.1007/BF02734606.
- [21] E. V. Gorbar and I. L. Shapiro, “Renormalization group and decoupling in curved space,” *JHEP* **02** (2003), 021 doi:10.1088/1126-6708/2003/02/021 [arXiv:hep-ph/0210388 [hep-ph]].
- [22] R. Kavanagh, “The one-loop correction to gravitons in de Sitter space induced by massive scalars,” Utrecht University Theses repository (2023), <https://studenttheses.uu.nl/handle/20.500.12932/45224>.
- [23] P. S. Galiza, “Transverse Green’s function in quantum gravity,” *Phys. Rev. D* **30** (1984), 2097-2099 doi:10.1103/PhysRevD.30.2097.
- [24] A. Platania, “Causality, unitarity and stability in quantum gravity: a non-perturbative perspective,” *JHEP* **09** (2022), 167 doi:10.1007/JHEP09(2022)167 [arXiv:2206.04072 [hep-th]].
- [25] J. F. Donoghue, “Nonlocal partner to the cosmological constant,” *Phys. Rev. D* **105** (2022) no.10, 105025 doi:10.1103/PhysRevD.105.105025 [arXiv:2201.12217 [hep-th]].
- [26] T. Appelquist and J. Carazzone, “Infrared Singularities and Massive Fields,” *Phys. Rev. D* **11** (1975), 2856 doi:10.1103/PhysRevD.11.2856.
- [27] A. M. Frolov and D. M. Wardlaw, “Analytical formula for the Uehling potential,” *Eur. Phys. J. B* **85** (2012), 348 doi:10.1140/epjb/e2012-30408-4 [arXiv:1110.3433 [nucl-th]].
- [28] B. Bertotti, L. Iess and P. Tortora, “A test of general relativity using radio links with the Cassini spacecraft,” *Nature* **425** (2003), 374-376 doi:10.1038/nature01997.
- [29] E. A. Uehling, “Polarization effects in the positron theory,” *Phys. Rev.* **48** (1935), 55-63 doi:10.1103/PhysRev.48.55.
- [30] D. Antypas, A. Banerjee, C. Bartram, M. Baryakhtar, J. Betz, J. J. Bollinger, C. Boutan, D. Bowering, D. Budker and D. Carney, *et al.* “New Horizons: Scalar and Vector Ultralight Dark Matter,” [arXiv:2203.14915 [hep-ex]].
- [31] P. Friedrich and T. Prokopec, “Entropy production in inflation from spectator loops,” *Phys. Rev. D* **100** (2019) no.8, 083505 doi:10.1103/PhysRevD.100.083505 [arXiv:1907.13564 [astro-ph.CO]].
- [32] J. W. Lee, “Brief History of Ultra-light Scalar Dark Matter Models,” *EPJ Web Conf.* **168** (2018), 06005 doi:10.1051/epjconf/201816806005 [arXiv:1704.05057 [astro-ph.CO]].
- [33] C. Boehm and P. Fayet, “Scalar dark matter candidates,” *Nucl. Phys. B* **683** (2004), 219-263 doi:10.1016/j.nuclphysb.2004.01.015 [arXiv:hep-ph/0305261 [hep-ph]].
- [34] D. Glavan, T. Prokopec and D. C. van der Woude, “Late-time quantum backreaction from inflationary fluctuations of a nonminimally coupled massless scalar,” *Phys. Rev. D* **91** (2015) no.2, 024014 doi:10.1103/PhysRevD.91.024014 [arXiv:1408.4705 [gr-qc]].
- [35] D. Glavan, T. Prokopec and A. A. Starobinsky, “Stochastic dark energy from inflationary quantum fluctuations,” *Eur. Phys. J. C* **78** (2018) no.5, 371 doi:10.1140/epjc/s10052-018-5862-5 [arXiv:1710.07824 [astro-ph.CO]].
- [36] E. Belgacem and T. Prokopec, “Quantum origin of dark energy and the Hubble tension,” *Phys. Lett. B* **831** (2022), 137174 doi:10.1016/j.physletb.2022.137174 [arXiv:2111.04803 [astro-ph.CO]].
- [37] E. Belgacem and T. Prokopec, “Spatial correlations of dark energy from quantum fluctuations during inflation,” *Phys. Rev. D* **106** (2022) no.12, 123514 doi:10.1103/PhysRevD.106.123514 [arXiv:2209.01601 [gr-qc]].
- [38] C. B. Adams, N. Aggarwal, A. Agrawal, R. Balafendiev, C. Bartram, M. Baryakhtar, H. Bekker, P. Belov, K. K. Berggren and A. Berlin, *et al.* “Axion Dark Matter,” [arXiv:2203.14923 [hep-ex]].